A Novel Fault Detection Method for an Integrated Navigation System using Gaussian Process Regression

Yixian Zhu[1,2], Xianghong Cheng[1,2] and Lei Wang[1,2]

[1](*School of Instrument Science and Engineering, Southeast University, China*)
[2](*Key Laboratory of Micro-Inertial Instrument and Advanced Navigation, China*)
(E-mail: xhcheng@seu.edu.cn)

For the integrated navigation system, the correctness and the rapidity of fault detection for each sensor subsystem affects the accuracy of navigation. In this paper, a novel fault detection method for navigation systems is proposed based on Gaussian Process Regression (GPR). A GPR model is first used to predict the innovation of a Kalman filter. To avoid local optimisation, particle swarm optimisation is adopted to find the optimal hyper-parameters for the GPR model. The Fault Detection Function (FDF), which has an obvious jump in value when a fault occurs, is composed of the predicted innovation, the actual innovation of the Kalman filter and their variance. The fault can be detected by comparing the FDF value with a predefined threshold. In order to verify its validity, the proposed method is used in a SINS/GPS/Odometer integrated navigation system. The comparison experiments confirm that the proposed method can detect a gradual fault more quickly compared with the residual chi-squared test. Thus the navigation system with the proposed method gives more accurate outputs and its reliability is greatly improved.

1. INTRODUCTION.   The navigation system provides navigation data, such as position, velocity and attitude information, which is delivered to a computer for guidance and control (Oh et al., 2005). Whether the navigation data is correct can affect the realization of accurate navigation. In order to improve the reliability and continuity of navigation, integrated navigation is used in many vehicles (Park et al., 2011). Since several sensors are used in an integrated navigation system, the correctness of sensor measurements directly affects the accuracy of navigation. Once a sensor fails, each subsystem will be contaminated by the fault after the multi-sensor information fusion and feedback. Therefore fault detection is essential to enhance the integrated navigation system's reliability and safety.

Due to the importance of fault detection, many researchers have devoted themselves to improving the reliability of systems. The existing fault detection methods can be broadly classified into three categories (Zhu and Hu, 2012): fault detection method based on an analytical model, fault detection method based on signal processing and fault detection method based on prior knowledge. Fault detection methods based on an analytical model process and diagnose the information under the assumption that the mathematic model of the system is known. Kalman filtering (Brumback and Srinath, 1987; Villez et al., 2011) and strong tracking filtering (Wang et al., 2004) are the most popular methods in this category. The filter is used to obtain the state estimation for fault prediction based on the analytical model of the system. If the predicted state is greater than the predefined threshold, a fault occurs. Brumback and Srinath (1987) constructed a chi-squared test statistic from the difference between two estimates based on a Kalman filter to realise real-time fault detection. On this basis, Joerger and Pervan (2013) put forward an improved method that can evaluate the probability that an undetected fault causes state estimate errors to exceed predefined bounds of acceptability. However, for some complex nonlinear systems, accurate models cannot be obtained. The other two categories of fault detection methods avoid this problem. Wavelet transformation (Jiang et al., 2003; Yan et al., 2014; Youssef, 2002) and Auto-Regressive Moving Average (ARMA) (Pham and Yang, 2010; Mohsen and Abu EI-Yazeed, 2004; Munoz, 2000) analyse the measured signal directly, and lead to fault detection methods based on signal processing. These methods detect the fault by extracting characteristic values from the signals such as variance, amplitude and frequency. Fault detection methods based on prior knowledge (Bacha et al., 2008; Mahadevan and Shah, 2009; Shabanian and Montazeri, 2011) have been drawing more and more attention because of their high intelligence. Bacha et al. (2008) realised automatic classification and fault severity degree evaluation by using a Neural Network (NN), of which the inputs were obtained using experimental data related to healthy and faulty machines. However, the dataset needed to train the NN is exceedingly large, which restricts the use of NN in practical application. By contrast, Support Vector Machine (SVM) is a novel learning method that requires only a small number of samples. Mahadevan and Shah (2009) used a feature selection and identified variables most closely related to the classification of normal and faulty data based on SVM. The outputs of SVM do not have probabilistic meaning. Fortunately, the newly developed Gaussian Process Regression (GPR) can overcome this drawback. It can provide not only the prediction corresponding to the unknown input but also the variance of the prediction (Huber, 2014). GPR has many advantages in solving problems in which the dataset has a high dimension or the size of the dataset is relatively small or the samples nonlinear.

This paper proposes a novel fault detection method for an integrated navigation system based on GPR. The Fault Detection Function (FDF), which is composed of the predicted innovation, the actual innovation of the Kalman filter and their variance, is presented. The innovative formula of FDF makes it sensitive to the faults, which is especially favourable to the detection of gradual faults. The GPR model, for the first time, is used to predict the innovation of the Kalman filter. In order to avoid local optimisation, particle swarm optimisation is applied to find the optimal values of GPR hyper-parameters. To highlight the advantages of the proposed method over the traditional method, contrast experiments are carried out. The results demonstrate that the proposed method can detect both abrupt faults and gradual faults effectively, which

greatly contributes to enhancing the accuracy and reliability of integrated navigation systems.

The paper is organised as follows: Section 2 introduces GPR assisted by particle swarm optimisation; Section 3 presents the fault detection algorithm based on GPR; Section 4 introduces SINS/GPS/Odometer (Strapdown Inertial Navigation System / Global Positioning System / Odometer) fault-tolerant system; Section 5 describes experimental results; and the last section is committed to concluding remarks.

2. GPR ASSISTED BY PARTICLE SWARM OPTIMISATION.

GPR was first proposed by Williams and Rasmussen (1995). It is a machine learning method developed from Bayesian theory and statistical theory. In mathematics, the GPR model is equivalent to many well-known models, such as spline model, Bayesian linear model and large artificial neural network.

A Gaussian Process (GP) is a collection of random variables, any finite number of which has a joint Gaussian distribution. A GP is completely specified by its mean function and covariance function (Williams and Rasmussen, 2006). The mean function $m(x)$ and the covariance function $k(x, x')$ of a real process $f(x)$ are defined respectively as

$$\begin{cases} m(x) = E[f(x)] \\ k(x,x') = E[(f(x) - m(x))(f(x') - m(x'))] \end{cases} \tag{1}$$

Then the GP is written as $f(x) \sim GP(m(x), k(x, x'))$.

The noisy version of the model is described as

$$y = f(x) + \varepsilon \tag{2}$$

where x denotes the input vector. $f(x)$ is the true value of function at location x. y is the observation polluted by noise. Assume that the noise ε observes Gaussian distribution: $\varepsilon \sim N(0, \sigma_n^2)$. Then the prior distribution of observation y, the joint prior distribution of observation y and function value f_* can be obtained as follows

$$y \sim N(0, K(X,X) + \sigma_n^2 I_n) \tag{3}$$

$$\begin{bmatrix} y \\ f_* \end{bmatrix} \sim N\left(0, \begin{bmatrix} K(X,X) + \sigma_n^2 I_n & K(X,x_*) \\ K(x_*,X) & k(x_*,x_*) \end{bmatrix}\right) \tag{4}$$

where the covariance matrix $K(X, X) = K_n = (k_{ij})$. The matrix element $k_{ij} = k(x_i, x_j)$ is used to measure the correlation between x_i and x_j. I_n denotes the n-dimensional unit matrix. n is equal to the column number of X. $K(X, x_*) = K(x_*, X)^T$ is the covariance matrix between training set input X and test point x_*. $k(x_*, x_*)$ is the covariance of test point x_* itself.

There are several covariance functions, among which square covariance is often used. The square covariance between x_i and x_j is written as

$$k(x_i,x_j) = \sigma_f^2 \exp\left(-\frac{1}{2}(x_i - x_j)^T M^{-1}(x_i - x_j)\right) \tag{5}$$

where $M = \text{diag}(l^2)$ is a diagonal matrix whose order is equal to the dimension of x_i. l is the scale of the variance. σ_f^2 denotes the variance of the single.

Then, the *posterior* distribution of function value f_* can be calculated as follows

$$f_*|X,y,x_* \sim N(\bar{f}_*, \text{cov}(f_*)) \tag{6}$$

where

$$\bar{f}_* = K(x_*,X)[K(X,X) + \sigma_n^2 I_n]^{-1}y \tag{7}$$

$$\text{cov}(f_*) = k(x_*,x_*) - K(x_*,X)[K(X,X) + \sigma_n^2 I_n]^{-1}K(X,x_*) \tag{8}$$

here $\bar{f}_*$ and $\text{cov}(f_*)$ are predictive mean and variance of function value f_* at location x_*, respectively.

There are some unknown parameters in Equations (7) and (8). In order to obtain these parameters, we define the hyper-parameter $\theta = \{l, \sigma_f^2, \sigma_n^2\}$. Finding the optimal values of the hyper-parameter is crucial to train a good prediction model. To overcome the problems of local optimal, Particle Swarm Optimisation (PSO) combined with the maximum likelihood method is proposed to determine the hyper-parameter.

Particle swarm optimisation was introduced by Kennedy and Eberhart (1995) and modified by Shi and Eberhart (1998). It came from the simulation of foraging behaviour of bird flocks and fish schools. As an evolutionary algorithm to obtain global optimisation, PSO can solve complex problems which are nonlinear or have multiple extremes.

Each particle represents a possible solution of the problem. The value of the objective function at a particle's position is defined as the fitness of the particle. The quality of a particle is measured by its fitness. Every particle remembers its own best position and the best position of its neighbours, which will be used when the particle changes its velocity. The PSO algorithm searches for the optimal solution by the cooperation and competition among individual particles.

Assume there is a swarm composed of N particles in D-dimensional search space. The position of particle i is written as $P_i = (p_{i1}\ p_{i2}\ ...p_{iD})^T$ and the velocity written as $V_i = (v_{i1}\ v_{i2}\ ...\ v_{iD})^T$, in which $i = 1, 2, ..., N$. The fitness of particle i is denoted as $f_p(P_i)$. $f_p(Pbest_i)$ and $Pbest_i = (pbest_{i1}\ pbest_{i2}\ ...\ pbest_{iD})^T$ are the personal best fitness and the personal best position of particle i, respectively. $f_p(Gbest)$ and $Gbest = (gbest_1\ gbest_2\ ...\ gbest_D)^T$ are the global best fitness and the global best position of the particle swarm, respectively. At the iteration m, the d-th dimensional velocity component v_{id}^m and position component p_{id}^m of particle i can be updated according to Equations (9) and (10), respectively.

$$v_{id}^{m+1} = \omega \cdot v_{id}^m + c_1 r_1(pbest_{id}^m - p_{id}^m) + c_2 r_2(gbest_d^m - p_{id}^m) \tag{9}$$

$$p_{id}^{m+1} = p_{id}^m + v_{id}^{m+1} \tag{10}$$

where m is the current iteration number. $d = 1, 2, ..., D$. $pbest_{id}^m$ and $gbest_d^m$ are the d-th dimensional component of the particle i's personal best position vector and the global best position vector at iteration m, respectively. $r_1, r_2 \in U(0,1)$ are random values. c_1 is the cognitive learning factor that represents the cognition that a particle has towards its own success. c_2 is the social learning factor that represents information sharing and cooperation between the particles. ω is the inertia weight that decides the impact of the previous velocity on the current velocity (Mahmoodabadi et al., 2012).

Based on the above theories, the algorithm to obtain the optimal values of the hyper-parameter is described as follows.

Step 1 Build the negative log marginal likelihood as

$$L(\theta) = -\log p(y|X, \theta)$$
$$= \frac{1}{2} y^T (K_n + \sigma_n^2 I_n)^{-1} y + \frac{1}{2} \log |K_n + \sigma_n^2 I_n| + \frac{n}{2} \log 2\pi \tag{11}$$

Step 2 Get the partial derivative of $L(\theta)$ on θ as

$$\frac{\partial L(\theta)}{\partial \theta} = \frac{1}{2} tr\left(\left((C^{-1}y) \cdot (C^{-1}y)^T - C^{-1} \right) \cdot \frac{\partial C}{\partial \theta} \right) \tag{12}$$

   where $C = K_n + \sigma_n^2 I_n$.

Step 3   Define the partial derivative as the fitness function of particle swarm optimisation to be minimised.

Step 3·1 Initialise velocities and positions of the particle swarm with random numbers in the search space.

Step 3·2 Calculate the fitness function of each particle.

Step 3·3 Compare each particle's fitness with its personal best fitness. If the current fitness is better, it will be set as the personal best fitness of the particle, and the current position set as the personal best position.

Step 3·4 Compare each particle's personal best fitness with the global best fitness of the particle swarm. If a personal best fitness is better, then set it as the global best fitness, and the position that corresponds to the global best fitness as the global best position.

Step 3·5 Update velocities and positions of the particles according to Equations (9) and (10).

Step 3·6 If the criterion is met, output the global best position as the optimal solution. Otherwise, go to Step 3·2.

The criterion is usually a sufficiently good fitness or a maximum number of iterations. Then the output global best position is just the optimal solution of hyperparameter θ.

3.   FAULT DETECTION ALGORITHM BASED ON GPR.   The error model of the system can be expressed as follows

$$X_k = \Phi_{k,k-1} X_{k-1} + W_{k-1} \tag{13}$$

where X_{k-1} is the error states of the integrated navigation system at time t_{k-1}, and X_k the error states at time t_k. $\Phi_{k,k-1}$ is the state transition matrix between time t_{k-1} and t_k. W_k is a zero mean white noise sequence with covariance Q_k.

The measurement equation of the system may be expressed as follows

$$Z_k = H_k X_k + V_k \tag{14}$$

where Z_k is the measurement differences at time t_k. H_k is the local filter measurement matrix. V_k is the measurement noise vectors with covariance R_k. W_k and V_k are assumed to be independent.
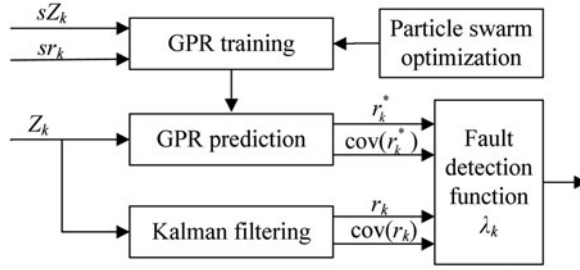
Figure 1. The functional diagram of the FDF construction.

Consider the system described by Equations (13) and (14). The functional diagram of the FDF construction is given in Figure 1. The FDF consists of two parts: the innovation of the Kalman filter and the predicted value of GPR model.

The time update of the Kalman filter defines the new estimate $\hat{X}_{k,k-1}$ of the state at time t_k based on the estimate at the previous time.

$$\hat{X}_{k,k-1} = \Phi_{k,k-1}\hat{X}_{k-1} \qquad (15)$$

where $\hat{X}_{k-1}$ is the estimate of the state at time t_{k-1}. Then the estimated measurement of the system can be calculated as follows

$$\hat{Z}_{k,k-1} = H_k\hat{X}_{k,k-1} \qquad (16)$$

The innovation of the Kalman filter is defined as

$$r_k = Z_k - \hat{Z}_{k,k-1} \qquad (17)$$

If there are no failures in the system before time t_{k-1}, the state estimate $\hat{X}_{k-1}$ at time t_{k-1} is correct. In this case, $\hat{Z}_{k,k-1}$ represents the estimated measurement of the system with no faults at time t_k. As a result, the innovation r_k is a Gaussian white sequence with zero mean as the system has no faults between time t_{k-1} and t_k. The covariance of the innovation r_k can be calculated as follows

$$\text{cov}(r_k) = H_k P_{k,k-1} H_k^T + R_k \qquad (18)$$

where $P_{k,k-1}$ denotes the expected value of the covariance matrix at time t_k predicted at time t_{k-1}. $P_{k,k-1}$ can be obtained at the Kalman filter prediction step.

At the same time, a GPR model is devoted to predicting the innovation of the Kalman filter. To build a GPR model, we need to have a dataset as a training sample. Some measurements and its corresponding Kalman filter innovations of the fault-free system, denoted by sZ_k and sr_k respectively, are taken as the training samples. Using the training samples sZ_k and sr_k, the GPR model is established through Steps 1–3 listed in Section 2. We train the GPR model based on finding the optimal value of hyper-parameter θ. By defining the partial derivative as the fitness function to be minimised, the PSO algorithm assists in finding the best setting of the GPR hyper-parameter. As the GPR model has been trained, it has the function of prediction. With the measurement Z_k as the input, the GPR model can predict
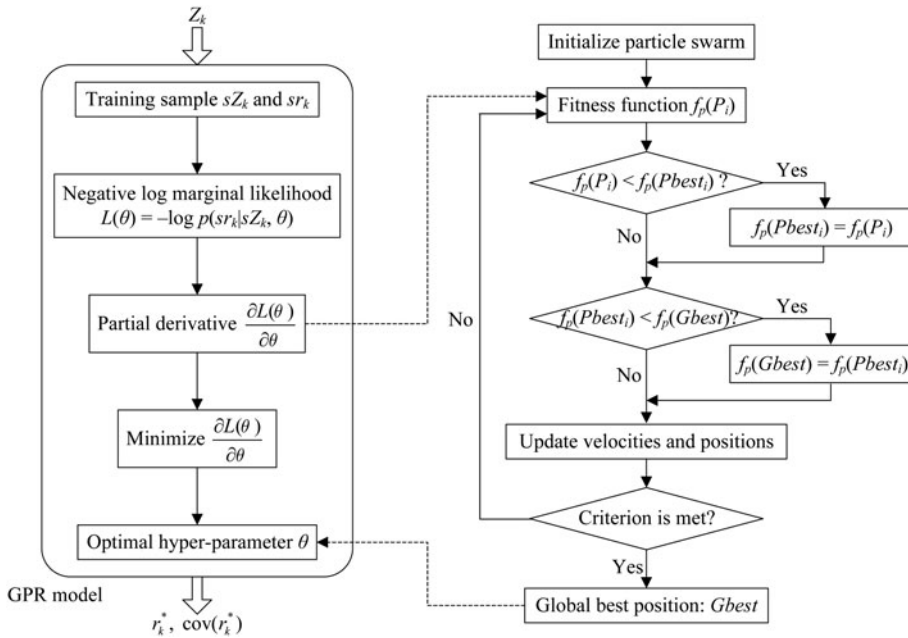
Figure 2. Particle Swarm Optimisation assists in training the GPR model.

the corresponding Kalman filter innovation r_k^* and give its covariance $\text{cov}(r_k^*)$ by Equations (7) and (8) respectively. Figure 2 shows the above description as a flow chart.

So far, we have got all the elements needed for constituting the FDF. On this foundation, we produce the definition of η_k, which is as follows

$$\eta_k = r_k - r_k^* \tag{19}$$

As the innovation r_k and the predicted innovation r_k^* are independent of each other, the covariance of η_k can be obtained as follows

$$A_k = \text{cov}(r_k) + \text{cov}(r_k^*) \tag{20}$$

If the system is operating normally, η_k is a Gaussian white sequence with zero mean. If a fault occurs, the mean of η_k is no longer equal to zero. Make assumptions about η_k as follows:

$$H_0 = \text{Fault-free} \quad \text{E}(\eta_k) = 0, \text{E}(\eta_k \cdot \eta_k^T) = A_k$$

$$H_1 = \text{Fault} \quad E(\eta_k) = \mu, E[(\eta_k - \mu) \cdot (\eta_k - \mu)^T] = A_k$$

Hence, there are the following conditional probability density functions:

$$P_r(\eta|H_0) = \frac{1}{\sqrt{2\pi} \cdot |A_k|^{1/2}} \exp(-\frac{1}{2}\eta_k^T A_k^{-1}\eta_k) \tag{21}$$

$$P_r(\eta|H_1) = \frac{1}{\sqrt{2\pi} \cdot |A_k|^{1/2}} \exp[-\frac{1}{2}(\eta_k - \mu)^T A_k^{-1}(\eta_k - \mu)] \tag{22}$$

where $|A_k|$ denotes the determinant of A_k.

Neyman-Pearson lemma shows the effectiveness of likelihood ratio test. We calculate the log likelihood rate of $P_r(\eta|H_1)$ and $P_r(\eta|H_0)$ as follows

$$\begin{aligned}\Lambda_k &= \ln \frac{P_r(\eta|H_1)}{P_r(\eta|H_0)} \\ &= \frac{1}{2}[\eta_k^T A_k^{-1}\eta_k - (\eta_k - \mu)^T A_k^{-1}(\eta_k - \mu)]\end{aligned} \tag{23}$$

The log likelihood rate Λ_k reaches its maximum when μ is equal to η_k. Then the FDF can be obtained as follows

$$\begin{aligned}\lambda_k &= \eta_k^T A_k^{-1}\eta_k \\ &= (r_k - r_k^*)^T \cdot [\text{cov}(r_k) + \text{cov}(r_k^*)]^{-1} \cdot (r_k - r_k^*)\end{aligned} \tag{24}$$

As a fault occurs, η_k is no longer a Gaussian white sequence with zero mean. The value of FDF λ_k will be bigger, which is used to detect the fault. The decision rule is given by the following

$$\begin{aligned}\lambda_k &> T_D &&\text{A fault has occurred} \\ \lambda_k &\leqslant T_D &&\text{No fault has occurred}\end{aligned}$$

where T_D is the threshold for detection. If the threshold value is too large, the probability of missed detection will increase. On the other hand, if the threshold value is too small, the probability of false alarm will increase. Therefore, we must measure the probability of false alarm and the probability of missed detection when determining the detection threshold.

4. SINS/GPS/ODOMETER FAULT-TOLERANT SYSTEM

4.1. *Fault-tolerant System Structure.* To improve the precision and reliability of the navigation system, multi-navigation system integrated schemes are the most popular at present. The integrated navigation composed of SINS, GPS and odometer is usually applied to land vehicles (Atia et al., 2014). SINS is an independent navigation system, which provides navigation parameters continually. Since the navigation error of SINS grows over time, assisting navigation approaches are needed to modify the cumulative error. As an assistant navigation observer, the odometer provides the velocity of the vehicle. GPS has high precision of positioning, but its reliability will decline owing to such factors as strong jamming and the blackout effect caused by obstructions.

While a number of methods for multi-sensor integration have been presented for navigation applications, the Kalman filter has proved to have the best performance.
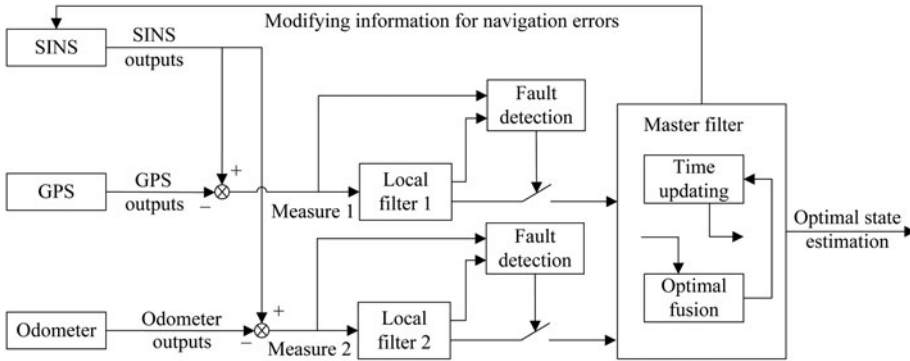
Figure 3. SINS/GPS/Odometer fault-tolerant system structure.

Therefore, the Kalman filter is applied to realise the local filter. The fault-tolerant structure of the SINS/GPS/Odometer integrated navigation system is given in Figure 3. SINS is the reference system. Two local filter systems are composed of GPS and odometer assisting SINS, respectively. The fault detection and isolation device is designed respectively for each local filter to detect and expose the subsystem fault in time, ensuring reliability of the navigation system. The FDF of local filter 1 indicates a fault in the GPS receiver, and that of local filter 2 indicates a fault in the odometer. When a fault is detected, the master filter no longer uses the output from the malfunctioning local filter. In other words, if a GPS receiver fault is detected, the SINS/GPS/Odometer integrated navigation system will be changed into a SINS/Odometer one. Similarly, if an odometer fault is detected, the SINS/GPS/ Odometer integrated navigation system will be changed into a SINS/GPS one. To ensure the system fault tolerance capability, the non-feedback federal filter is adopted to fuse the information of the subsystems. There is no feedback from the master filter to the local filter, which ensures the best fault tolerance capability. The master filter fuses the fault-free local filter information, and then outputs the optimal state estimation. Navigation error is estimated by the federal filter, and then fed back to the SINS.

4.2. *System Model.*   Set the East-North-Up (ENU) geographic coordinate as the navigation frame (*n*-frame), and the Right-Front-Up (RFU) frame as the body frame (*b*-frame). Take the 15-dimensional error state vector as the state variable of the integrated navigation system, namely

$$X_k = [\begin{array}{ccccccccccccccc} \phi_e & \phi_n & \phi_u & \delta V_e & \delta V_n & \delta V_u & \delta L & \delta\lambda & \delta h & \varepsilon_x & \varepsilon_y & \varepsilon_z & \nabla_x & \nabla_y & \nabla_z \end{array}]^T$$

where ϕ_e, ϕ_n, ϕ_u are attitude errors. δV_e, δV_n, δV_u are velocity errors. δL, $\delta\lambda$, δh are position errors. ε_x, ε_y, ε_z are gyroscope drifts. ∇_x, ∇_y, ∇_z are accelerometer biases.

GPS and odometer assist SINS independently, constituting local filter 1 and local filter 2, respectively. The two local filters estimate the state variable according to the observed data. The measurement equations of the two local filters can be described

respectively as

$$Z_k^{(1)} = \begin{pmatrix} L_{SINS} - L_{GPS} \\ \lambda_{SINS} - \lambda_{GPS} \end{pmatrix} = H_k^{(1)} X_k^{(1)} + V_k^{(1)} \tag{25}$$

$$Z_k^{(2)} = \begin{pmatrix} V_{eSINS} - V_{eOd} \\ V_{nSINS} - V_{nOd} \end{pmatrix} = H_k^{(2)} X_k^{(2)} + V_k^{(2)} \tag{26}$$

where the subscript *SINS, GPS* and *Od* denote SINS output, GPS receiver output and odometer output, respectively. L, λ, V_e and V_n are latitude, longitude, east velocity and north velocity of the vehicle, respectively. $X_k^{(1)} = X_k$. $X_k^{(2)} = X_k$. $V_k^{(1)}$ and $V_k^{(2)}$ are the measurement noise vectors with covariance $R_k^{(1)}$ and $R_k^{(2)}$ respectively. $H_k^{(1)}$ and $H_k^{(2)}$ are the local filter measurement matrices which take the following form

$$H_k^{(1)} = \begin{pmatrix} 0_{2\times6} & I_{2\times2} & 0_{2\times7} \end{pmatrix} \tag{27}$$

$$H_k^{(2)} = \begin{pmatrix} 0_{2\times3} & I_{2\times2} & 0_{2\times10} \end{pmatrix} \tag{28}$$

where $I_{2\times2}$ is a 2×2 identity matrix. $0_{2\times6}$, $0_{2\times7}$, $0_{2\times3}$ and $0_{2\times10}$ are zero matrices with different orders.

Since the non-feedback federal filter is used, the master filter itself has no information distribution and no filtering operation. The only responsibility of the master filter is to fuse the local state estimates. The fusion algorithm can be described as follows

$$P_k^g = [(P_k^{(1)})^{-1} + (P_k^{(2)})^{-1}]^{-1} \tag{29}$$

$$\hat{X}_k^g = P_k^g \cdot [(P_k^{(1)})^{-1} \cdot \hat{X}_k^{(1)} + (P_k^{(2)})^{-1} \cdot \hat{X}_k^{(2)}] \tag{30}$$

where $\hat{X}_k^g$ denotes the optimal estimation. $\hat{X}_k^{(1)}$ and $\hat{X}_k^{(2)}$ are the estimates of the error states obtained from local filter 1 and local filter 2, respectively. $P_k^{(1)}$ and $P_k^{(2)}$ are the covariance matrixes of $\hat{X}_k^{(1)}$ and $\hat{X}_k^{(2)}$, respectively. P_k^g is the covariance matrix of $\hat{X}_k^g$.

5. EXPERIMENTS AND RESULTS. To evaluate the proposed detection method, experiments have been carried out. Figure 4 shows the experimental vehicle system that includes IMU, GPS receiver, odometer and navigation computer. Pictures of the IMU and odometer are presented in Figure 5. The reference system is an integrated navigation system consisting of a navigation-grade IMU and a GPS receiver. The reference system provides precise navigation results as reference values. The test navigation system for evaluating the proposed method is composed of a GPS receiver, an odometer and a low-cost IMU. The two systems share the GPS receiver. Field tests were carried out in Beijing in a wide-open area, where satellite signals were easy to receive.

To verify the proposed fault detection method, fault information is set artificially by adding a gradual fault, an abrupt fault and an outlier into the measurements of the GPS receiver. A gradual fault is usually caused by increasing measurement noise, small biases or drifts in the signal over time. An abrupt fault may happen when the GPS satellite signals are unavailable for a short time. An outlier is a single point with a large error at a sampling time, which sometimes appears in a GPS receiver. It

Figure 4. The experimental vehicle system.

Figure 5. IMU and odometer.

is worth noting that the simulated fault in the GPS receiver is only added to the measurements of the test navigation system rather than the reference system. The total time of the test was 900 seconds. Fault information is set up as shown in Table 1.

Based on the above experimental setup, experiments have been performed. Figure 6 shows the position trajectories of the integrated navigation system with different operations. The vehicle travelled from point A to point B. The position trajectory of the system without fault detection has significant errors compared with the reference position trajectory. These large position errors are caused by the added faults in the GPS receiver. When the abrupt fault and the outlier occur, the trajectories of the system with the two methods are pretty close. This reveals that the two methods behave similarly when they deal with the abrupt fault and the outlier. The trajectory of the system with residual chi-squared method deviates from the reference position when the gradual fault occurs. Then as the fault has been detected, the position errors have been reduced gradually. However, under the same experimental conditions, the position curve of the system with the proposed method is almost coincidental with that of the reference system. Thus it can be seen that the proposed method detected all the added faults effectively.

Table 1. Setting faults for GPS receiver.

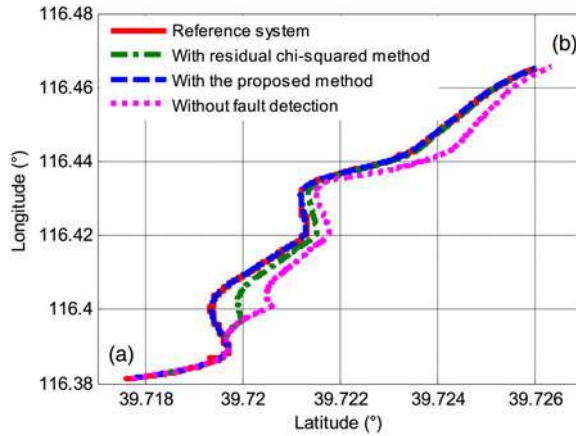| Fault types	Fault value	Time(s)
Gradual fault	2 m/s	100–200
Abrupt fault	500 m	580–600
Outlier	350 m	700

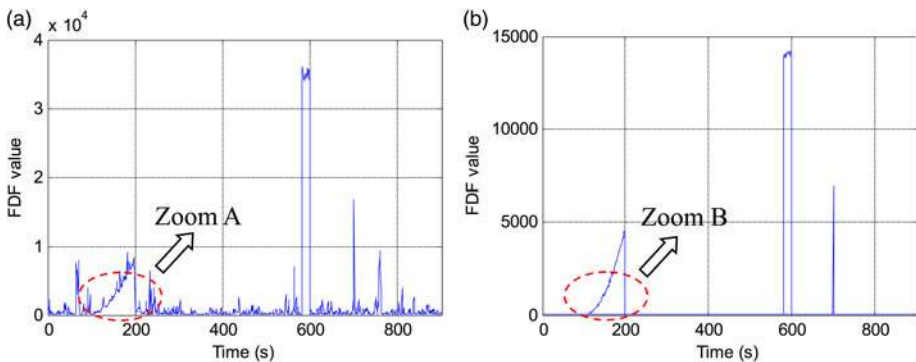Figure 6. Position trajectories.

Figure 7. FDF of GPS receiver. (a) Using residual chi-squared test. (b) Using the proposed method.

To further illustrate the performance of the proposed fault detection method, detailed comparisons have been made between the residual chi-squared test and the proposed method. Figure 7 shows the fault detection function (FDF) of GPS receiver obtained by the residual chi-squared test and the proposed method respectively. FDF reflects the magnitude of fault. The greater the fault, the higher the FDF value will be. A comparison of Figure 7(a) and Figure 7(b) reveals that the FDFs obtained from the two methods are in the same order of magnitude as a fault occurs. However, when there
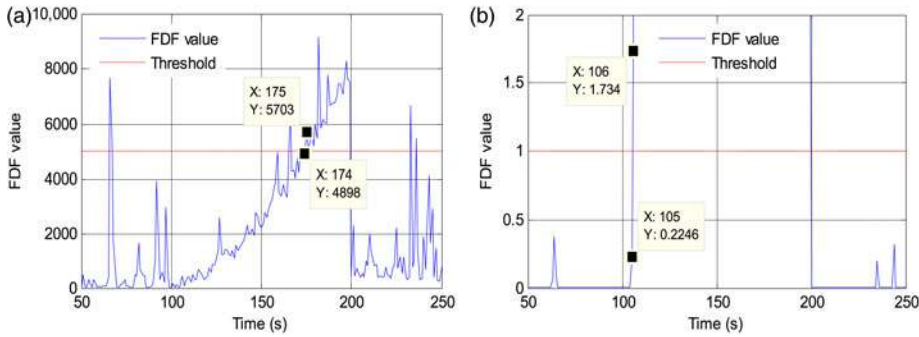
Figure 8. Drawings of partial enlargement. (a) Zoom A. (b) Zoom B.

Table 2. Comparison of detection results.

Times	Residual chi-squared test	Proposed method
False alarm	19	0
Missed detection	73	5

is no fault, the FDFs are on different scales. During the fault-free period, the FDFs of the two methods are mostly in the order of 10^3 and 10^{-3} respectively. This shows that the FDF of the proposed method has a more obvious jump in value than that of the residual chi-squared test when a fault occurs.

The large difference between the FDF value of the fault-free system and that of the failing system benefits the detection of gradual faults. To confirm this point, further comparison and analysis are made. Taking the detection of the gradual fault for the GPS receiver as an example, the FDFs obtained from the two methods are locally amplified, corresponding to Zoom A and Zoom B as shown in Figure 8. Taking the probability of false alarm and missed detection into consideration, the threshold of the residual chi-squared test and that of the proposed method are assigned the values of 5000 and 1 respectively. The threshold of the proposed method is small, thanks to the low FDF value of the fault-free system. Figure 8(a) shows that the FDF value is higher than the predefined threshold starting at the 175th second. So the residual chi-squared test has a delay of 74 s when it is used to detect the gradual fault. As Figure 8(b) shows, the threshold of the proposed method is so small that it is sensitive to the change of FDF value. At time $t = 106$ s, the FDF value is 1·734 which is greater than the predefined threshold 1. The delay time is 5 s, which is much less than that of the residual chi-squared. Less time delay in detection means lower probability of missed detection. Thus it can be seen that the probability of missed detection of the proposed method has considerably diminished. By comparing Figures 8(a) and 8(b), it is clear that the times of false alarms of the residual chi-squared are significantly more than that of the proposed method. The detailed comparison of detection results is shown in Table 2, which further validates the above analysis.

Figure 9 shows the position errors obtained by the two methods. In Figure 9(a), the position errors are outside the normal range from the moment that the gradual fault is
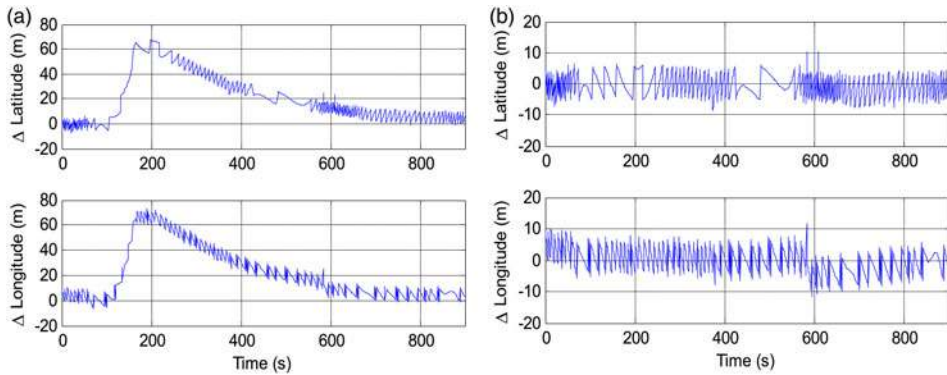
Figure 9. Position errors. (a) Using residual chi-squared test. (b) Using the proposed method.

added to the measurements of the GPS receiver. The reason for this phenomenon is that the gradual fault is not detected until the time t = 175 s. Once the fault is detected, the measurements of the GPS receiver will not be delivered to the master filter anymore until the FDF value is lower than the threshold again. Then the position errors will be corrected gradually by the SINS/Odometer integrated navigation. Figure 9(b) shows the smooth position errors with a precision of 10 m. It is once again verified that the proposed method can detect all the added faults in time, thereby avoiding the defects that the faults have on the navigation results.

6. CONCLUSIONS. As a guarantee to system reliability, fault detection of the integrated navigation system draws extensive attention. This paper proposes a novel fault detection method based on GPR. In order to avoid the local optimisation, particle swarm optimisation combined with maximum likelihood method is introduced to find the optimal hyper-parameters of the GPR model. FDF is made up of the prediction of GPR, the innovation of the Kalman filter and their variance. Experiments for a SINS/GPS/Odometer integrated navigation system to which the proposed method is applied demonstrate that the method can detect both abrupt faults and gradual faults effectively. Furthermore, the comparison experiments show the FDF of the proposed method is more sensitive to faults than that of the residual chi-squared test, which enhances the advantages of the proposed method. Therefore the system using the proposed method offers more accurate navigation information.

REFERENCES

Atia, M. M., Karamat, T. and Noureldin, A. (2014). An enhanced 3D multi-sensor integrated navigation system for land-vehicles. *The Journal of Navigation*, **67**(4), 651–671.

Brumback, B. D. and Srinath, M. D. (1987). A chi-square test for fault-detection in Kalman Filters. *IEEE Transactions on Automatic Control*, **32**(6), 552–554.

Bacha, K., Henao, H., Gossa, M. and Capolino, G. A. (2008). Induction machine fault detection using stray flux EMF measurement and neural network-based decision. *Electric Power Systems Research*, **78**(7), 1247–1255.

Huber, M. F. (2014). Recursive Gaussian process: On-line regression and learning. *Pattern Recognition Letters*, **45**, 85–91.

Jiang, J. A., Fan, P. L. and Chen, C. S. (2003). A fault detection and fault-phase selection approach for transmission lines with Haar wavelet transform. *IEEE PES Transmission and Distribution Conference and Exposition*, Dallas, USA, 285–289.

Joerger, M. and Pervan, B. (2013). Kalman filter-based integrity monitoring against sensor faults. *Journal of Guidance, Control and Dynamics*, **36**(2), 349–361.

Kennedy, J. and Eberhart, R. (1995). Particle swarm optimization. *IEEE International Conference on Neural Networks*, Perth, Australia, 1942–1948.

Mohsen, A. A. K. and Abu EI-Yazeed, M. F. (2004). Selection of input stimulus for fault diagnosis of analog circuits using ARMA model. *International Journal of Electronics and Communications*, **58**(3), 212–217.

Munoz, A. R. (2000). Using an autoregressive model in the detection of abnormal characteristics of squirrel cage induction motors. *Electric Power Systems Research*, **55**(2), 73–77.

Mahadevan, S. and Shah, S. L. (2009). Fault detection and diagnosis in process data using one-class support vector machines. *Journal of Process Control*, **19**(10), 1627–1639.

Mahmoodabadi, M. J., Bagheri, A., Nariman-zadeh, N. and Jamali, A. (2012). A new optimization algorithm based on a combination of particle swarm optimization, convergence and divergence operators for single-objective and multi-objective problems. *Engineering Optimization*, **44**(10), 1167–1186.

Oh, S. H., Hwang, D. H., Park, C., Lee, S. J. and Kim, S. H. (2005). Attitude determination GPS/INS integrated navigation system with FDI algorithm for a UAV. *Journal of Mechanical Science and Technology*, **19**(8), 1529–1543.

Park, S. G., Jeong, H. C., Kim, J. W., Hwang, D. H. and Lee, S. J. (2011). Magnetic compass fault detection method for GPS/INS/Magnetic Compass integrated navigation systems. *International Journal of Control, Automation, and Systems*, **9**(2), 276–284.

Pham, H. T. and Yang, B. S. (2010). Estimation and forecasting of machine health condition using ARMA/GARCH model. *Mechanical Systems and Signal Processing*, **24**(2), 546–558.

Rasmussen, C. E. and Williams, C. K. I. (2006). *Gaussian Processes for Machine Learning*. MIT Press, London.

Shabanian, M. and Montazeri, M. (2011). A neuro-fuzzy online fault detection and diagnosis algorithm for nonlinear and dynamic systems. *International Journal of Control, Automation, and Systems*, **9**(4), 665–670.

Shi, Y. H. and Eberhart, R. (1998). A modified particle swarm optimizer. *IEEE International Conference on Evolutionary Computation*, Anchorage, USA, 69–73.

Villez, K., Srinivasan, B. and Rengaswamy, R. (2011). Kalman-based strategies for Fault Detection and Identification (FDI): Extensions and critical evaluation for a buffer tank system. *Computers & Chemical Engineering*, **35**(5), 806–816.

Wang, D., Zhou, D. H. and Jin, Y. H. (2004). A strong tracking predictor for nonlinear processes with input time delay. *Computers & Chemical Engineering*, **28**(12), 2523–2540.

Williams, C. K. I. and Rasmussen, C. E. (1995). Gaussian processes for regression. *Proc. of the 9th Annual Conference on Neural Information Processing Systems*, Denver, USA, 514–520.

Yan, R. Q., Gao, R. X. and Chen, X. F. (2014). Wavelets for fault diagnosis of rotary machines: A review with applications. *Signal Processing*, **96**, 1–15.

Youssef, O. A. S. (2002). New algorithm to phase selection based on wavelet transforms. *IEEE Transactions on Power Delivery*, **17**(4), 908–914.

Zhu, D. Q. and Hu, Z. (2012). *Fault Diagnosis and Fault Tolerant Control of Underwater Robots*. National Defense Industry Press, Beijing.